Plate 4.2: Typical examples of basic volcanics from the Doornpoort Formation (Farm Du Plessis Rus 537) and its equivalents in the Dordabis area (Farm Ibenstein 55).

(A) Photomicrograph of amygdaloidal basalt showing large, epidote-filled amygdales in an intergranular matrix; plane polarized light.

(B) Clast supported flow top breccia displaying angular and subrounded clasts of amygdaloidal basalt in a matrix of fine-grained quartz arenite; coin for scale (diameter 38 mm).

(C) Photomicrograph illustrating the intergranular texture of basalt from a massive domain, here the inner part of a flow. Large crystals of plagioclase (pl) are intergrown with abundant opaque minerals (hematite and magnetite) and subordinate chlorite and epidote; crossed Nicols.

(D) Photomicrograph of fractured basalt from a permeable domain. The fractures are quartz-filled and the fine-grained intergranular basalt has been epidotised; plane polarized light.

(E) Photomicrograph of basalt displaying an intergranular texture. The plagioclase crystals have been completely replaced by epidote, quartz, calcite and chlorite during alteration. The metamorphic replacement was a static event and did not affect original crystal shapes (compare Plate 4.2 C); plane polarized light.

(F) Altered (epidotised) basalt from the Klein Aub area showing two generations of fractures. An earlier generation of fine, anastomosing, epidote-filled fractures (1) is associated with penetrative epidotisation of the basalt. These fractures are truncated by later tension gashes which are filled with fibrous quartz; coin for scale (diameter 38 mm).

Plate 4.2

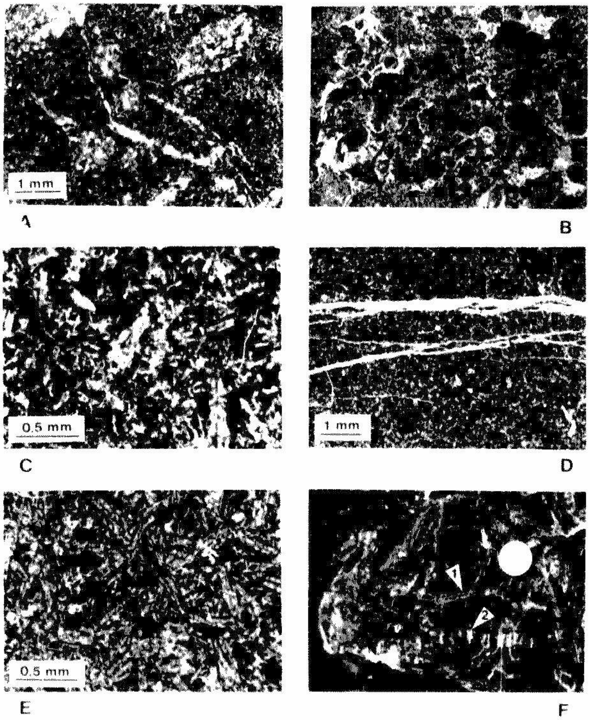

characterizes the second group of basalt, which accounts for approximately 25% of the basalts of the Sinclair Sequence. Permeability has been provided by primary features such as flow top breccias, sediment-filled cooling (contraction) fractures and amygdaloidal zones (Plate 4.2,A,B). Other permeable features were tectonically induced and are zones of secondary, tectonically induced permeability, e.g. shear zones, faults, tension gashes (Plate 4.2,D) and hydraulic fractures. The mineralogical composition of the basalts from permeable domains differs strongly from that of the massive basalt. Although primary basaltic textures are retained, the rocks consist of epidote (50%), quartz (15%), chlorite and subordinate calcite, dolomite, muscovite, and hematite and the basalt does not contain any plagioclase (Plate 4.2,E). Fractures are filled with quartz, epidote, calcite and locally dolomite. In the Klein Aub area, an early set of epidote- and quartz-filled fractures is associated with penetrative epidotisation of the surrounding basalt. The fractures are intersected by a later set of extensional fractures filled by fibrous quartz, which apparently did not interact with the basalt (Plate 4.2,F).

Since the amygdales contain a wide variety of commonly submicroscopically intergrown alteration products, their contents were additionally analysed. XRD-analyses determined that quartz, dolomite, calcite, epidote, chlorite, pumpellyite, laumontite and in some rare cases malachite, azurite, cuprite and native copper occur as fillings of amygdales in the basalt. The macroscopical occurrence of some of these minerals is indicated on the log of borehole ODB 4 (Fig.4.2) but no systematic vertical zonation of metamorphic minerals, that might reflect a systematic change in metamorphic grade, as described from the Portage Lake Volcanics, Michigan (Jolly, 1974), has been identified.

No fresh, unmetamorphosed basalt is preserved within the Kalahari Copperbelt. Compared with the basalts from permeable domains which have been affected to a much stronger extent by (hydrothermal) alteration the massive basalts, and which still contain plagioclase, these basalts are simply referred to as unaltered.

4.4.2 Geochemical Characteristics

Concentrations of major- and trace-elements in basalts from the Klein Aub and Dordabis areas have been determined by XRF-analyses. These data are shown in Appendix II, but characteristic elements have been plotted in bar graphs (Fig.4.12) and 'Isocon'-diagrams (Fig.4.13) to determine their mobile or immobile behaviour during metamorphic alteration. Element distributions, shown in bar diagrams, have been used to distinguish altered from unaltered basalts. However, this method does not distinguish between small changes in element concentrations either due to alteration or a change in volume. Grant (1986) introduced the Isocon method diagram, and it was used to define the overall concentration changes. The method can be applied where element concentrations in unaltered (C^O) and altered rocks (C^A) can be compared and is a graphic solution which considers composition-volume relations in alteration processes based on an equation proposed by Gresens (1967). In an Isocon diagram (Fig.4.13), the absolute concentration of an element is multiplied by any factor to fit it comfortably within the range of the diagrams scale. Such scaling is mathematically valid and prevents the underestimation of elements less abundant than silica or alumina. It also allows the determination of the absolute concentration of all elements directly from the diagram, by amplifying the scale-value with the factor given with the element. Values for major elements are given in percent, trace elements in ppm and PGE and Au in ppb. A reference line, corresponding to a zero concentration change (the 'isocon'), is determined by a best fit to the data. The slope of the isocon, compared with that of no mass change (45° slope) defines the mass change during alteration. After the definition of this isocon, gains, losses or immobility of elements in relation to the original rock can be determined. The basalts from massive domains have what are considered normal base metal contents for this rock type (120ppm Zn, 70ppm Co, 90 ppm Cu) when compared with data given by Wedepohl (1978); (Table 2). Only Pb and Fe values appear to be anomalously high.

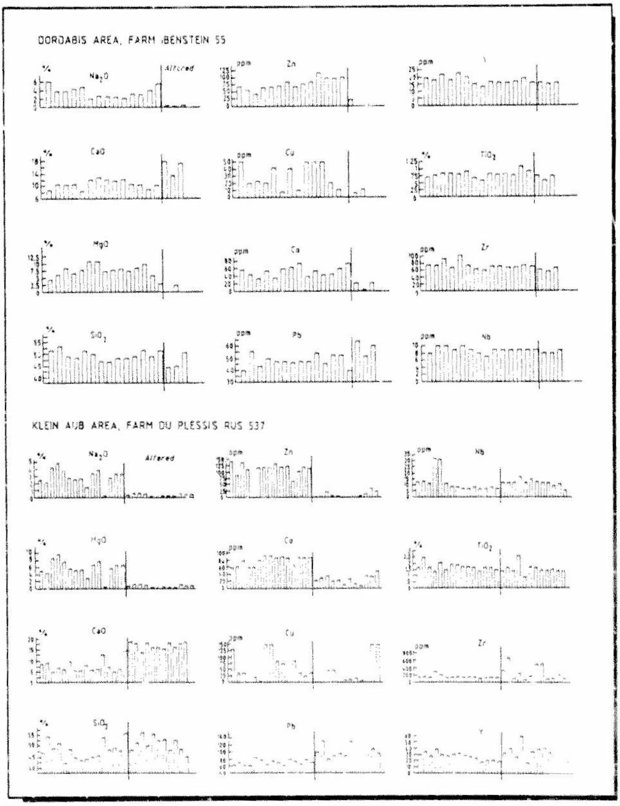

Fig.4.12: Bar diagrams of mobile and immobile elements in unaltered (left of black bar) and altered basalts (right of black bar) of the Doornpoort Formation and equivalents

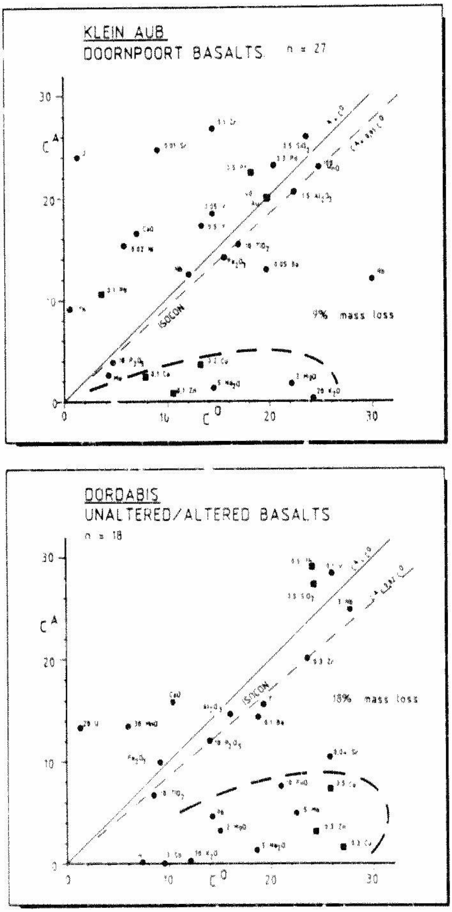

Fig.4.13: Isocon diagrams comparing original element concentrations (C^O; unaltered) with element concentrations in altered basalts (C^A) of the Doornpoort Formation and equivalents (method after Grant, 1986). The diagrams illustrate the strong depletion of base metals and "pathfinder"-elements (Na, Mg, K) and the contrasting behaviour of Pb, Au, Pt, Pd during alteration (no PGE and Au concentrations for Dordabis basalts determined). See text for explanation of method.

	Basalt	Granite	Rhyolite
Cu	100	15	5
Co	45	5	1
Zn	120	75	100
Pb	5	30	30
Ag	0.12	0.04	0.05

Table 2: Typical metal concentrations in source rocks from various provenances (after Wedepohl, 1978). Note that the concentrations of metals (except Pb) in basalt are approximately one order of magnitude higher compared with the other rock types. Thus the basalts represent the best potential source rock of the three examples given.

Basalts from permeable, epidotised domains have suffered a loss in volume of 8% in the Klein Aub area and 18% in the Dordabis area. These rocks are chemically characterised by their total depletion in Na, Mg and K and an enrichment in Ca (Figs.4.12, 4.13). Whereas Cu, Zn and Co are strongly depleted in the epidotised basalts, Pb and U show a significant enrichment. Cu values show a rather irregular distribution pattern whi[illegible] due to a 'nugget effect' produced by infrequently scattered specks of native Cu on m[illegible]actures. Precious metals such as Au, Pt and Pd (data only available for the Klein Aub area), have remained immobile or show a slight enrichment in the epidotised basalts which will be discussed in more detail in Chapter 8. The elements Ti, Zr, Y, Al and Nb have remained immobile during metamorphism and subsequent hydrothermal events (Figs.4.12, 4.13).

4.4.3 Interpretation of Alteration Patterns

The basalts were hydrothermally altered during regional metamorphism and show mineral assemblages typical of lower greenschist facies grade. Experimental studies of the stability fields of pumpellyite suggest a temperature range from 200°C to 300°C for metamorphism (Heinrichsen and Schurmann, 1969). This approximation of the temperature of metamorphism is supported by the absence of biotite in the metamorphic mineral assemblage. Such a range of metamorphic temperatures is also in agreement with metamorphic temperatures of less than 350°C, derived from illite crystallinity studies by Ahrendt et al. (1978).

Original Pb contents seem to have been anomalously high, possibly reflecting characteristics of the regional metal province. Pb, together with U and possibly Th, Au, Pt and Pd were enriched during metamorphic alteration. Other base metals, such as Cu, Zn, and Co, were heavily leached during the same alteration event with minor amounts of Cu precipitated in fractures and amygdales, whereas Zn and Co were completely remobilised from the volcanic pile. The total amount of Cu leached from the epidotised domains exceeds the amount of native Cu found in the altered basalt. It is important to note, that approximately 25% of the basalts are estimated to have been depleted in most of their original Cu, Zn and Co contents, despite rare occurrences of native Cu.

Other elements such as K, Na, and Mg, have been dramatically remobilised during alteration and are used as chemical pathfinder elements for the metal depletion. Since it occurs in carbonates in amygdales and fractures, introduced Ca contents correlate well with the permeability of the altered basalts.

Similar processes of basalt alteration and leaching of base metal have been described from numerous areas, e.g. the Keweenawan rift, Michigan (Jolly, 1974), Western Australia (Haynes, 1972) and Alaska (Sood et al., 1986). In each case the metal depleted basalts have been affected by metamorphic alteration and are associated with sporadic occurrence of native copper. In the previously mentioned locations extensive strata-bound Cu mineralization is fo[illegible] in sediments overlying leached basalts.

4.4.4 Timing of Alteration

The alteration, epidotisation and base metal depletion of the Sinclair basalts is related to features of primary permeability and to tension gashes, shear zones and faults. Although no detailed structural study on these basalts has been undertaken, it appears that induced permeability is related to folding and faulting of the Damaran Orogeny.

The rather erratic and somewhat depleted copper concentrations of the massive basalt might be due to earlier metal depletion, and is interpreted to have occurred shortly after extrusion and along flow top breccias. However, no mineralogical evidence was found for such an early alteration, but evidence could have been destroyed during regional metamorphism. Since no other base metals show signs of such an earlier event, it appears likely that the erratic distribution of Cu is due to a localized 'nugget effect'.

The quartz-filled extensional fractures, which cut across the earlier epidote veins, represent a subordinate tectothermal event that post-dates the Damaran Orogeny. Preliminary, unpublished fluid inclusion studies show, that the quartz crystals contain only one generation of inclusions, commonly displaying negative quartz crystal shapes, which are interpreted as primary inclusions (G.Schneider, pers. com. 1987). The fluids have a low salinity (4.5% NaCl-equivalent) and show homogenisation temperatures of 175°C. Cracking temperatures determined by decrepitometer in one sample of milky vein quartz from Klein Aub Mine were obtained by A.Schmidt-Mumm (pers. com., 1985) and the cracking temperatures showed a maximum at 350°C. A subordinate peak indicated an additional thermal event with temperatures of approximately 160°C. This peak at 350°C corresponds well with the maximum temperature of 350°C from an illite crystallinity study of the Southern Foreland of the Damara Orogen (Ahrendt et al., 1978).

Although the results from the fluid inclusion study are only preliminary and results from the decrepitometer method have to be used very carefully, it seems that the rocks of the Sinclair Sequence have undergone a second weaker thermal event, subsequent to regional metamorphism. Since metal solubilities at such salinities and temperatures are relatively low and the wall rocks show no signs of any interaction with these fluids, it is inferred that no basalt alteration was associated with this subordinate event.

5. SEDIMENTARY ROCKS OF THE SINCLAIR SEQUENCE

5.1 Doornpoort Formation

The Doornpoort Formation consists of approximately 3000 m of coarse-grained clastic sediments with intercalations of tholeiitic basalt at the base (Fig.5.1). The lithofacies distribution within the Sinclair Sequence has been studied along 23 sections across the stratigraphy in the Klein Aub area (Figs.5.2, 5.3, Appendix I). The following sedimentary facies types have been identified. The following description of the various lithofacies types is arranged in order of decreasing grain size.

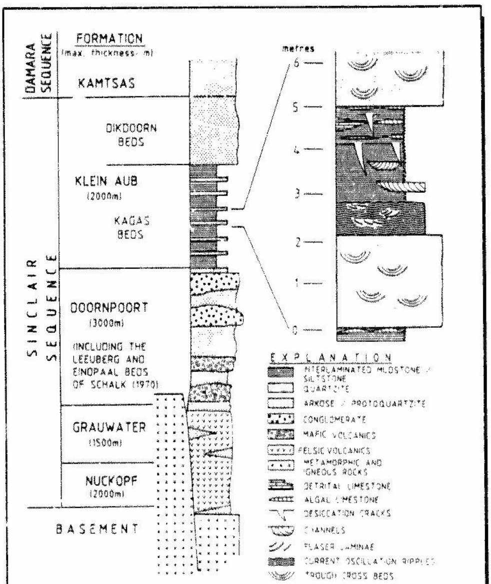

Fig.5.1: Stratigraphy of the Sinclair Sequence in the study area.

5.1.1 Conglomerate and Arkose Facies

The conglomerate and arkose facies as a whole varies from 100 m to 800 m in thickness (Fig.5.2). It displays lensoid geometries with lenses 10-20 km across and 500 m maximum thickness on average. The facies also occurs as a minor component of the Nuckopf Formation whereas it makes up approximately 50% of the Grauwater Formation. In both formations the lithofacies is interbedded with felsic volcanics. The facies is most extensively developed in the

Doornpoort Formation, where it is interbedded with the protoquartzite facies. This widespread development is associated with an overlapping beyond the previously deposited formations and an overstepping of the graben margins, exemplified locally by the covering of basement horst structures (Fig.5.2). This heterolithic lithofacies is composed of 0.5 m-2.5 m thick conglomerate beds and is interbedded with arkosic beds 0.1-10 m in thickness. The conglomerates consist of poorly sorted, matrix-supported, sub-angular to sub-rounded clasts averaging 8 cm, but clasts up to 70 cm in diameter have been observed (Plate 5.1,A). The matrix is arkosic and is mineralogically and texturally immature. The conglomerates are generally massive and show no obvious imbrication features. Some units show both normal and inverse grading with largest clasts in the middle of the unit. The clasts are derived from both extrabasinal and intrabasinal sources. Clasts derived from the older Proterozoic basement include granite, granodiorite, vein quartz, subordinate dolerite and minor banded iron formation. Local clasts derived from within the depository include red quartz porphyry and quartz-feldspar porphyry from the Nückopf and Grauwater Formations. Protoquartzite and arkose clasts of these formations are also present, but as a minor constituent.

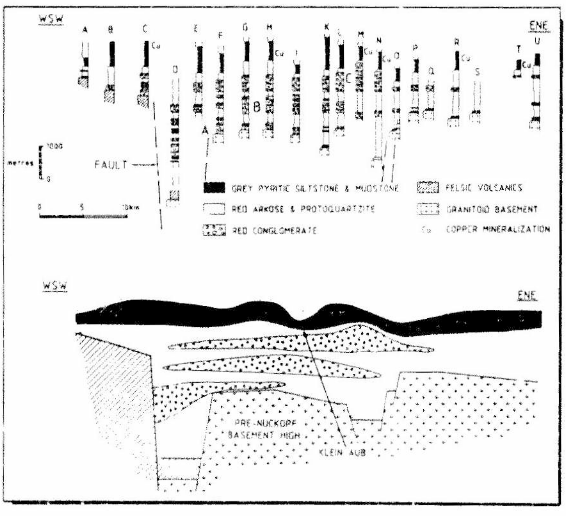

Fig.5.2: (A) Measured sections A-U through the Doornpoort and Klein Aub Formations; (B) Correlation diagram showing distribution of lithotypes. N.B. the *en echelon* arrangement of alluvial fan lenses.

The interbedded arkose beds are 15-100 cm thick and comprise coarse sandstones to granulestones which commonly contain scattered pebbles of vein quartz. The arkose beds are texturally as well as mineralogically immature. Both planar cross-stratification and rare trough cross-bedding are developed that average 80 cm in thickness, as well as planar lamination

Palaeocurrents were directed to the south and southwest in agreement with measurements of Ruxton (1981, 1986). The arkose units are lensoid and of short lateral extent. Within the Doornpoort Formation of the study area there are three major conglomerate lenses developed and one of them forms the basal conglomerate directly overlying the basement. The lenses are arranged in an *en echelon* fashion with their maximum thicknesses shifting progressively towards the east (Fig.5.2).

One lens of alluvial fan conglomerate is exceptionally well exposed on Farm Eindpaal 516, 4 km east of Klein Aub Mine (Fig.5.4) In Figure 5.2 measured sections A-U represent a longitudinal profile parallel to the edge of the basin. In these sections the interbedded conglomerate and arkose facies is well represented. Measured sections U-X, however, are situated around the Witkop Anticline (Fig.5.3) and allow an important opportunity to examine basinward facies distribution. In these sections the facies is poorly developed and the conglomeratic lenses have thinned considerably and reduced in number.

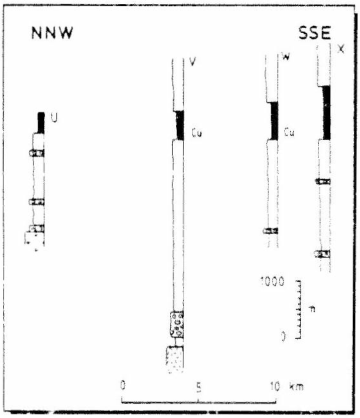

Fig.5.3: Measured section U-X through the Doornpoort and Klein Aub Formations. The arrangement of these sections differs from the ones in Fig.5.2 in that they represent a profile from the basin margin towards deeper parts of the basin.

Interpretation: The matrix-supported nature of the conglomerates and the absence of sedimentary structures suggest that they were deposited by debris flow processes. Conversely, the arkosic units show well developed sedimentary structures and their immature nature suggests that they were transported subaqueously and deposited on bedforms including sand waves, dunes and plane beds. The presence of debris flows and the lensoid geometry of the facies indicates that the units represent a southward progradation of individual alluvial fans. The rapid decrease in the thickness and percentage of the facies southward indicates that the fans were developed proximal to the source area. The interbedded arkoses represent sheetflood and braided stream deposits laid down between successive debris flow events. The cyclic arrangement of the conglomeratic units indicates repeated fault activity and uplift in the source area

Plate 5.1:

(A) Interbedded conglomerate and arkose facies of the Doornpoort Formation. Note the massive nature of the conglomerate and the plane lamination of the arenite (hammer is 1 m long)

(B) Polygonal desiccation cracks within the fine-grained sandstone/siltstone facies developed in playa lakes (diameter of coin 17 mm).

(C) Fining-upward cycles of the Kagas Beds in the Klein Aub Formation in a river section 4 km east-north-east of Klein Aub Mine. Base and top of one complete cycle are arrowed. The person is sitting on the quartz arenite facies which represents deposits from subtidal to lower tidal flat environment. Above this are facies representing lower to upper tidal flat deposits.

(D) Shallow sand-filled channel (basal scour (1)) within the interlaminated and flaser laminated facies (same locality as Fig.5.1,C). Laminae may represent small-scale epsilon cross-stratification filling this channel, with reactivation surfaces developed (2).

(E) A progression from interlaminated subfacies (1) to flaser laminated subfacies (2) developed on the mid tidal flat (same locality as Plate 5.1,C). The more easily eroded flaser laminated subfacies is eroded to form a mid tidal flat channel (3) which is sand-filled. This area subsequently became a zone of active deposition of sand beds (4).

(F) Close-up photograph of same facies details shown in 5.1, E.

(G) Sand-filled large desiccation crack (upper arrow) developed in the interlaminated facies (same facies as in Plate 5.1,C). A thin lensoid algal limestone is also indicated (lower arrow). It displays a cellular structure and is interpreted as intertidal algal mats (coin is 17 mm in diameter). **(H)** Detail of algal laminated facies intercalated with the mid-tidal flat deposits (same locality as Plate 5.1,C). Plane laminated limestone passes upwards into poorly developed stromatolitic domes.

Plate 5.1